A713T Supplemental Information

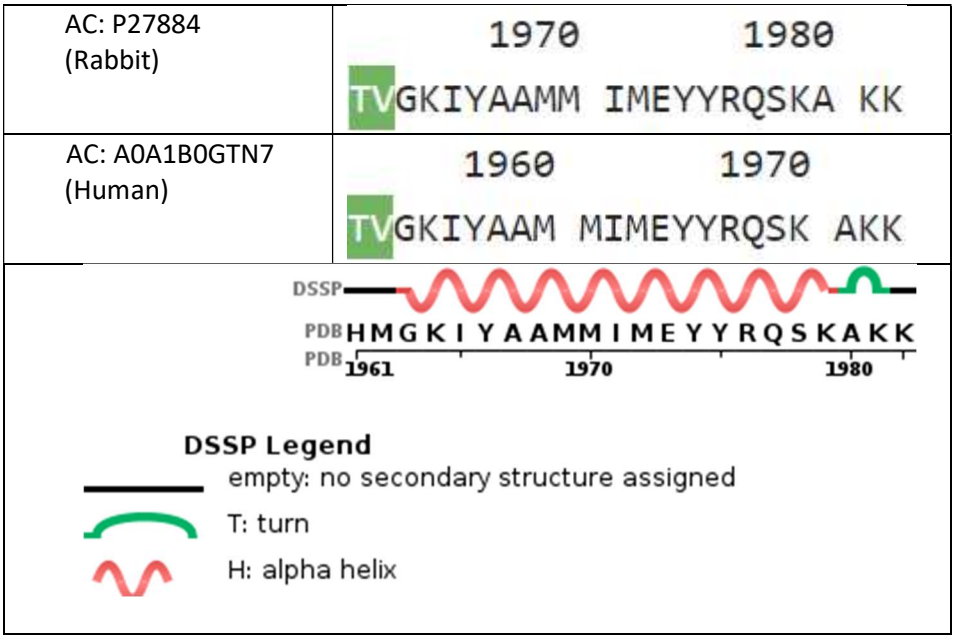

Figure S1. Residues in crystal structure of Cav2.1 IQ domain PDB ID: 3DVM different than Human and Rabbit Cav2.1 sequence. The first 2 residues of the 22 residue crystal structure by Kim et al. do not match. The first two residues are HM in the crystal structure (bottom image) while the first 2 residues under Uniprot Accession IDs P27884 and A0A1B0GTN7 (as well as O00555; figure not shown) are TV (top 2 images).

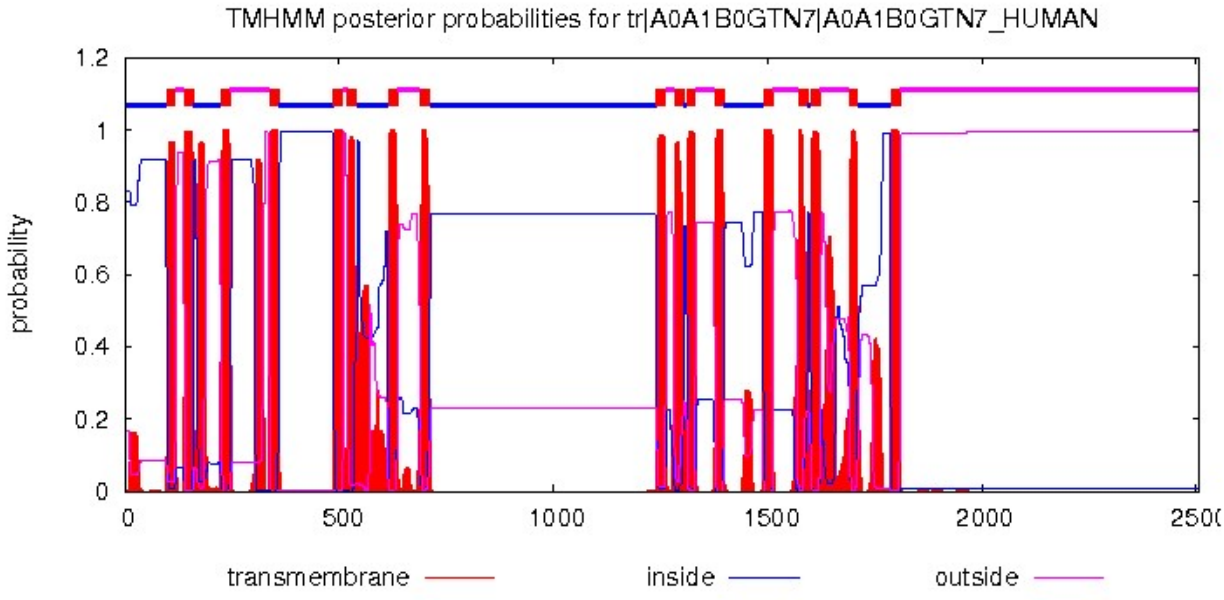

Figure S2. TMHMM 2.0 accurately predicts TM domains of Cav2.1. Despite missing a few of the TM S3 and S4 helices (data not shown), this tool was accurate in predicting the four TM domains of Cav2.1.

A

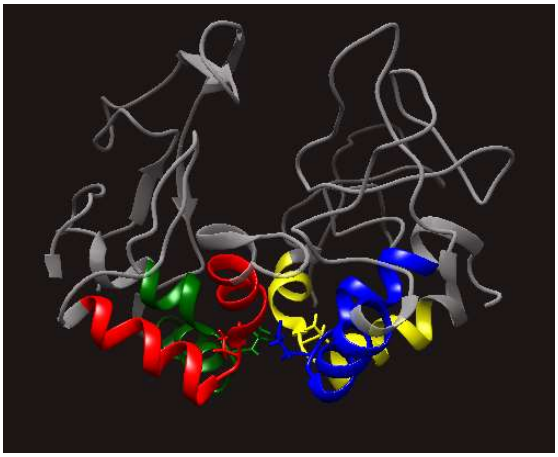

B

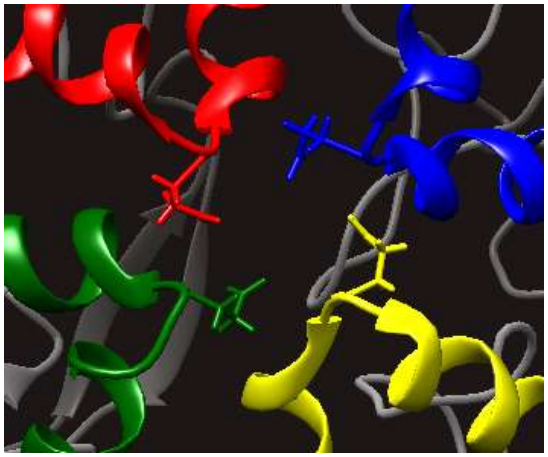

C

TM1	280-301	1	FSMLTVYQCITMEGWTDVLY 20
			|::|||:||||||||:||
	249-335	58	FAVLTVFQCITMEGWTDLLY 77
TM2	602-623	2	ALISVFQVLTGEDWNSVMYNG 22
			|:::|||:||||||.|||:|
	637-689	21	AIMTVFQILTGEDWNEVMYDG 41
TM3	1001-1021	1	LSAMMSLFTVSTFEGWPQLL 20
			|.|:::||||||.||||:|
	1398-1484	50	LWALLTLFTVSTGEGWPQVL 69
TM4	1312-1330	1	AVLLLFRCATGEAWQEILL 19
			|::||||.|||||..|:|
	1711-1782	35	ALMLLFRSATGEAWHNIML 53

Figure S3. P-loops motifs of the S5-S6 linker in Rabbit Cav1.1 (PDB ID 6BYO). A) The reentrant P-loops between S5 and S6. Each P-loop for all four domains is colored in a different color. B) Looking up from cytoplasm, the four P-loop glutamic acid residues E292, E614, E1014, & E1323 of Rabbit Cav1.1 that coordinate the pore of HVA channels C) align to residues E318, E668, E1460, & E1756 respectively in Human Cav2.1 (accession A0A1B0GTN7) using Smith-Waterman algorithm (Rabbit Cav1.1 top, Human Cav2.1 bottom). Molecular graphics and analyses performed with UCSF Chimera, developed by the Resource for Biocomputing, Visualization, and Informatics at the University of California, San Francisco, with support from NIH P41-GM103311. [Data from from Cardozo & Martinez-Ortiz 2017, PDB ID 6BYO]

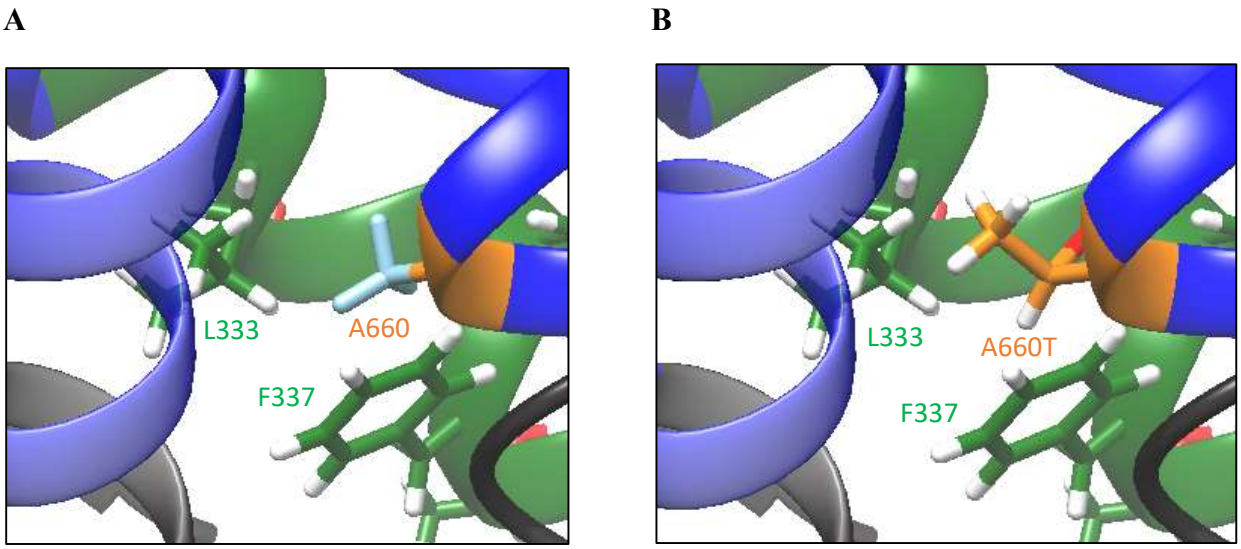

Figure S4. Interaction between I-II linker and alanine residue in Rabbit Cav1.1 that aligns with Cav2.2 A713. A) This figure contains the crystal structure Rabbit Cav1.1 (PBD ID 6KZO) showing the alanine residue at the bottom of the IIS6 helix and the residues in the vicinity from the I-II linker domain which have been studied in relation to VDI in high-voltage activated (HVA) channels. The blue helices are the S6 regions and the conserved alanine in HVA channels A660 residue at bottom of IIS6 is in orange while the linker I-II cytosolic region is in green with L333 and F337 residues labelled. B) Same image as in A however we show the mutant threonine residue in replacement of the conserved alanine. Molecular graphics and analyses performed with UCSF Chimera, developed by the Resource for Biocomputing, Visualization, and Informatics at the University of California, San Francisco, with support from NIH P41-GM103311. [Data from Zhao et al., 2019, Nature 576: 492-497, PDB ID 6KZO and from Cardozo & Martinez-Ortiz 2017, PDB ID 6BYO]

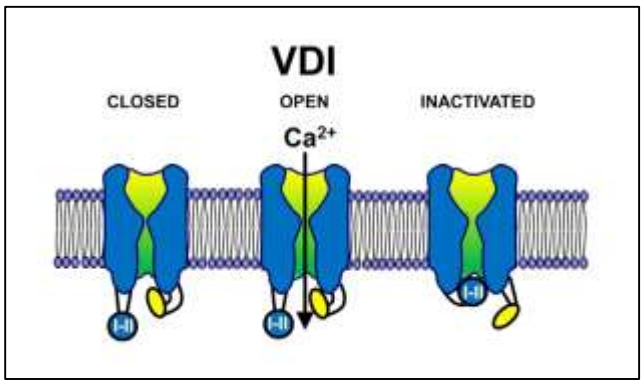

Figure S5. The "hinge-lid" transmembrane domain I-II linker VDI mechanism of HVA channels. This image shows the hypothesized mechanism of voltage-dependent inactivation (VDI) for Cav1 and Cav2 channels. The inactivation gate (blue I-II ball) docks at the pore entry to the cytoplasmic domain to block Ca^{2+} entry. Image taken from Simms & Zamponi, Neuronal Voltage-Gated Calcium Channels: Structure, Function, and Dysfunction. 2014.

```
FT   HELIX           81..99
FT                   /evidence="ECO:0000244|PDB:6KZP"
FT   TURN            103..107
FT                   /evidence="ECO:0000244|PDB:6KZP"
FT   HELIX           112..135
FT                   /evidence="ECO:0000244|PDB:6KZP"
FT   HELIX           152..171
FT                   /evidence="ECO:0000244|PDB:6KZP"
FT   STRAND          177..179
FT                   /evidence="ECO:0000244|PDB:6KZP"
FT   HELIX           180..189
FT                   /evidence="ECO:0000244|PDB:6KZP"
FT   HELIX           190..193
FT                   /evidence="ECO:0000244|PDB:6KZP"
FT   HELIX           195..207
FT                   /evidence="ECO:0000244|PDB:6KZP"
FT   HELIX           208..211
FT                   /evidence="ECO:0000244|PDB:6KZP"
FT   HELIX           212..233
FT                   /evidence="ECO:0000244|PDB:6KZP"
FT   STRAND          236..242
FT                   /evidence="ECO:0000244|PDB:6KZP"
FT   STRAND          245..247
FT                   /evidence="ECO:0000244|PDB:6KZO"
FT   TURN            251..253
FT                   /evidence="ECO:0000244|PDB:6KZO"
FT   TURN            264..266
```

Figure S6. Except from UniProtKB with secondary structure used by ClustalW2 secondary structure algorithm. This SWISS-PROT entry format for Human Cav3.1 (accession ID O43497) can be accessed from the UniProt entry by selecting “Format” > “Text”. The secondary structure FT entries of HELIX, STRAND, and TURN are parsed by ClustalW2 and a set of sequences or another profile can be aligned using these structures as a guide. Results from alignment can be seen in Figure 14B of main paper. Note that secondary structure annotations in UniProt can come from multiple PDB IDs indicated in yellow.

A

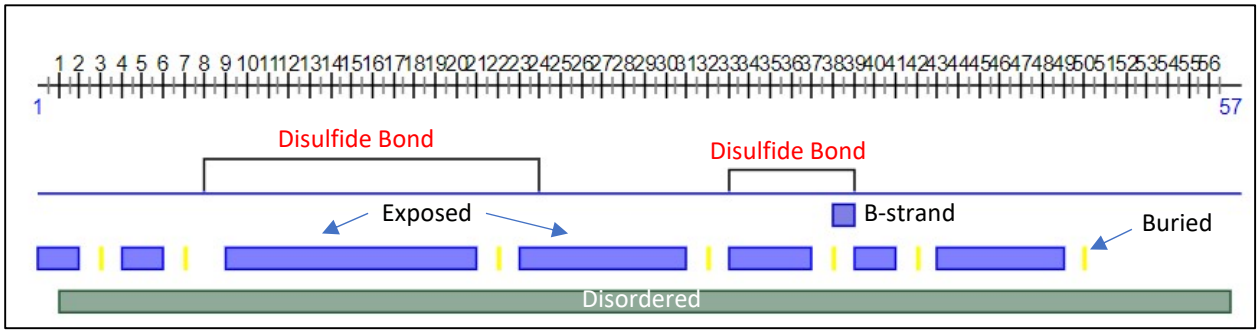

B

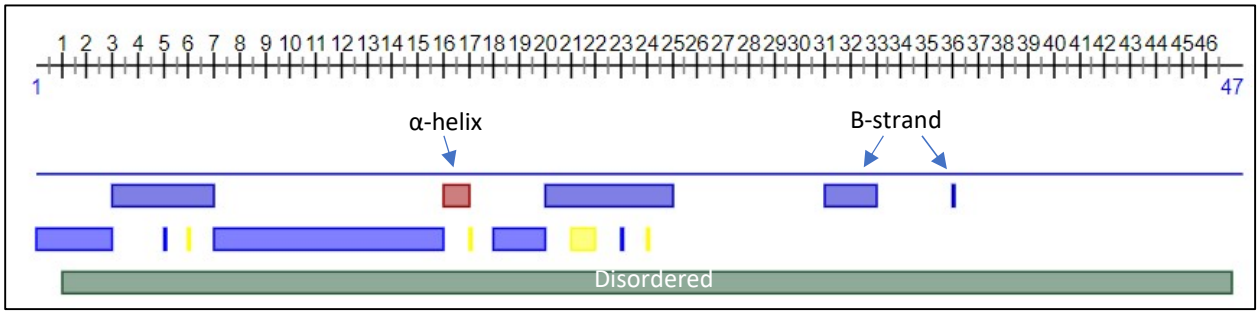

Figure S7. PredictProtein secondary structure predictions of aligned EC linker regions of Human Cav2.1 for A) linker region of Cav2.1 between IS5 and IS6 N-terminal to respective P-loop and B) linker region of Cav2.1 between IIIS5 and IIIS6 also N-terminal to respective P-loop. Predictions show mostly exposed residues as well as disordered regions. β-strands are predicted for IIIS5/S6 linker as well as an alpha helix that is unlikely. These are same spans from alignment with Rabbit Cav1.1 in Figure 15 of main paper.